ACS APPLIED MATERIALS & INTERFACES

Research Article

www.acsami.org

Perovskite $Sr_{1-x}Ce_xCoO_{3-\delta}$ ($0.05 \leq x \leq 0.15$) as Superior Cathodes for Intermediate Temperature Solid Oxide Fuel Cells

Wei Yang,[†,‡] Tao Hong,[§] Shuai Li,[†,‡] Zhaohui Ma,[†,‡] Chunwen Sun,[†,‡,*] Changrong Xia,[§,*] and Liquan Chen[†,‡]

[†]Beijing National Laboratory for Condensed Matter Physics, Institute of Physics, Chinese Academy of Sciences, Beijing 100190, China

[‡]Key Laboratory for Renewable Energy, Chinese Academy of Science, Beijing Key Laboratory for New Energy Materials and Devices, Beijing 100190, China

[§]CAS Key Laboratory for Materials for Energy Conversion, Department of Materials Science and Engineering, University of Science and Technology of China, Hefei 230026, China

ABSTRACT: Perovskite $Sr_{1-x}Ce_xCoO_{3-\delta}$ ($0.05 \leq x \leq 0.15$) have been prepared by a sol–gel method and studied as cathodes for intermediate temperature solid oxide fuel cells. As SOFC cathodes, $Sr_{1-x}Ce_xCoO_{3-\delta}$ materials have sufficiently high electronic conductivities and excellent chemical compatibility with SDC electrolyte. The peak power density of cells with $Sr_{0.95}Ce_{0.05}CoO_{3-\delta}$ is 0.625 W cm^{-2} at 700 °C. By forming a composite cathode with an oxygen ion conductor SDC, the peak power density of the cell with $Sr_{0.95}Ce_{0.05}CoO_{3-\delta}$-30 wt %SDC composite cathode, reaches 1.01 W cm^{-2} at 700 °C, better than that of $Sm_{0.5}Sr_{0.5}CoO_3$-based cathode. All these results demonstrates that $Sr_{1-x}Ce_xCoO_{3-\delta}$ ($0.05 \leq x \leq 0.15$)-based materials are promising cathodes for an IT-SOFC.

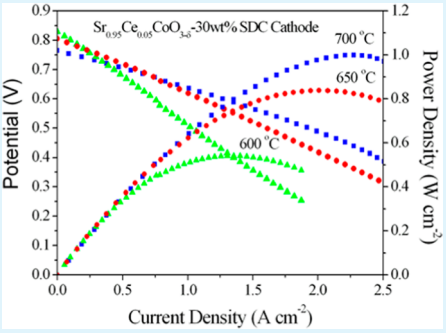

KEYWORDS: *solid oxide fuel cell, oxygen-reduction reaction, $Sr_{1-x}Ce_xCoO_{3-\delta}$, composite cathode, intermediate temperature*

1. INTRODUCTION

Solid oxide fuel cells (SOFCs) are the most attractive among all kinds of fuel cells, especially considering the fuel flexibility and high energy conversion efficiency due to high operating temperatures.[1,2] However, high operation temperature puts harsh requirements on SOFCs component materials and thus leads to rapid degradation of the cells. Therefore, great efforts have been devoted to lowering the operating temperature to intermediate temperature range of 600–800 °C or even lower.[2] However, reducing the operating temperature decreases the electrode kinetics and results in large interfacial polarization resistances as well. This effect is most pronounced for the oxygen reduction reaction (ORR) at the cathode.[3] In recent years, much attention has been paid to modification of the conventional cathode materials and searching for new materials that can efficiently work at intermediate or low temperature ranges.

Cobalt containing perovskite $SrCoO_{3-\delta}$ has attracted much attention as potential cathode materials for oxygen permeation and SOFCs because of its high electrochemical activity, however, $SrCoO_{3-\delta}$ is unstable, chemically and thermally incompatible with yttria-stabilized zirconia (YSZ), samaria/gadolinia-doped ceria (SDC/GDC) and lanthanum strontium gallium magnesium oxide (LSGM) electrolytes. Doping on A-site or/and B-site were usually adopted to stabilize $SrCoO_{3-\delta}$ and reduce the thermal expansion coefficient (TEC). Although iron partially substituting of cobalt successfully limits the phase transition of $SrCoO_{3-\delta}$ and does reduce the thermal expansion coefficient of $SrCoO_{3-\delta}$ down to the appropriate level of the commonly used electrolytes, oxygen vacancy ordering arised from ferrite-doping deteriorates its electrochemical performance. Partially substituting Sr with Ba to form $Ba_{0.5}Sr_{0.5}Co_{0.8}Fe_{0.2}O_3$ (BSCF) suppresses the oxygen vacancy ordering process and shows excellent electrochemical performance at intermediate temperature,[4] but it is reactive to CO_2 and water.[5,6] Therefore, the design of an efficient and stable cathode for ORR at intermediate temperature is still a major challenge to the construction of IT-SOFCs.

James et al.[7] studied structure and magnetism in the oxygen-deficient perovskites $Sr_{1-x}Ce_xCoO_{3-\delta}$ (hereafter abbreviated as SCCO). Maignan et al.[8] found that the most metallic composition of $Sr_{1-x}Ce_xCoO_{3-\delta}$ corresponds to $x = 0.05$ and $\delta \approx 0.28$. Wei et al. studied the electrical properties of $SrCoO_{3-\delta}$ doped by CeO_2.[9] It was found that the conductivity of $Sr_{1-x}Ce_xCoO_{3-\delta}$ enhanced with increasing CeO_2 within the solubility limit. The conductivity over 500 S cm^{-1} was obtained at $x = 0.15$ when testing at 350–400 °C for the sample sintered at 1100 °C. To the best of our knowledge, there is no report on the electrochemical performance of SCCO as a cathode for solid oxide fuel cells so far. In this work, we investigated

Received: November 30, 2012
Accepted: January 21, 2013
Published: January 21, 2013

   dx.doi.org/10.1021/am3029238 | ACS Appl. Mater. Interfaces 2013, 5, 1143–1148

perovskite $Sr_{1-x}Ce_xCoO_{3-\delta}$ ($0 < x \leq 0.2$) and their composites with SDC as cathode materials for immediate temperature SOFCs. For the composition of $x = 0.2$ in SCCO, the sample has low electronic conductivity due to more CeO_2 impurity. So we only present the results of three compositions $Sr_{1-x}Ce_xCoO_{3-\delta}$ ($x = 0.05$, 0.10, and 0.15) in this paper.

2. EXPERIMENTAL SECTION

2.1. Synthesis of $Sr_{1-x}Ce_xCoO_{3-\delta}$ ($x = 0.05$, 0.10, 0.15). In a typical sol–gel synthesis of $Sr_{1-x}Ce_xCoO_{3-\delta}$ ($x = 0.05$, 0.10, 0.15), stoichiometric amounts of AR-grade strontium nitrate ($Sr(NO_3)_2$), cobalt nitrate ($Co(NO_3)_2{\cdot}6H_2O$), and cerium nitrate ($Ce(NO_3)_3{\cdot}6H_2O$) were dissolved in 100 mL of distilled water. Then, 2.31 g of citric acid were dissolved in a solution consisting of 8 mL of ethylene glycol (EG) and 10 mL of distilled water, and added to the above solution with uniformly mixed; a pink solution was obtained. After stirring the solution for 10 h at 80 °C on a hot plate, the solution became a stiff gel. The brown gel was dried in an electric oven at 250 °C to obtain a dark-gray precursor. Then the precursor was pelleted and calcined at 1100 °C in air for more than 72 h followed by repeatedly grinding, pelleting, and calcining until no further reactions were detected.

2.2. Characterizations. X-ray powder diffraction (XRD) patterns were recorded in a Philips X'Pert PRO diffractometer equipped with Cu Kα radiation over the 2θ range of 20–80° or 10–130° for each sample, and refinement of the SCCO structure was conducted using a GSAS-EXPGUI software[10] with PowderX for data preparation.

Chemical compatibility between SCCO and SDC was examined by mixing SCCO and SDC in a weight ratio of 1:1 and calcining for 5 h at 1000 °C and then checked by X-ray diffraction test.

Thermogravimetric analysis (TGA) profiles were collected with a NETZSCH STA 449C high-temperature thermoanalyzer apparatus (Netzsch Inc., Germany) at a heating/cooling rate of 2.5 °C/min from 20 to 900 °C in air. About 130 mg of the $Sr_{0.95}Ce_{0.05}CoO_{3-\delta}$ sample was used in the TGA experiment. Thermal mechanical analysis (TMA) was employed for the measurement of the thermal expansion coefficient with a NETZSCH DIL 402C apparatus and with an Al_2O_3 reference in the temperature range of 17.5–1000 °C and a ramp rate of 5 °C min^{-1} in air.

Electronic conductivity of SCCO samples were measured in temperature range of 400 to 800 °C using a 4-probe configuration with a Keithley 2400 SourceMeter (Keithley Instruments, Inc.). The relative density of the bar-shaped samples is about 83%, measured with Archimedes method.

2.3. Fabrication and Testing of Cells. The electrochemical performance of SCCO as intermediate temperature SOFC cathodes was characterized with a samaria-doped ceria ($Sm_{0.2}Ce_{0.8}O_{1.9}$, SDC)-based symmetric cell and a single cell. A symmetric cell was fabricated by uniaxial pressing 300 mg highly porous SDC powder obtained by a glycine-nitrate combustion process[11] at 500 MPa and sintering for 5 h at 1400 °C, SCCO powder was thoroughly mixed with ethyl cellulose and terpinol, the cathode paste was painted symmetrically on the both sides of the electrolyte followed by sintering at 900–1000 °C for 2 h, Ag paste was painted subsequently on the SCCO cathodes as a current collector.

SDC-based single cells were fabricated by a dry-pressing procedure, using highly porous SDC and NiO powder prepared by a glycine-nitrate method and calcined at 600 °C for 2 h and 850 °C for 4 h, respectively. For a single cell, the mixture of SDC, NiO, graphite with a weight ratio of 35: 65: 20 was pressed at 200 MPa to form a green anode support, SDC powder was then added, uniformly distributed and copressed onto the obtained green support pellet at 300 MPa. The resultant green half cells were then calcined at 1300 or 1350 °C for 5 h; SCCO cathode was painted onto both sides of the SDC electrolyte in a symmetric cell, then dried and sintered at 950 °C. Ag paste was subsequently painted onto the cathode as a current collector.

The polarization resistances of the symmetric cells were determined by electrochemical impedance using IM6e (Zahner) from 600 to 700 °C in a frequency range of 0.1 Hz to 1 M Hz.

Single cell was first reduced in wet hydrogen (3 vol.% H_2O) at 600 °C and tested in humidified hydrogen and air from 600 to 700 °C with an interval of 50 °C using a SOLARTRON electrochemical workstation.

3. RESULTS AND DISCUSSION

3.1. Structure and Chemical Compatibility. Figure 1 shows the XRD patterns of the as-synthesized $Sr_{1-x}Ce_xCoO_{3-\delta}$

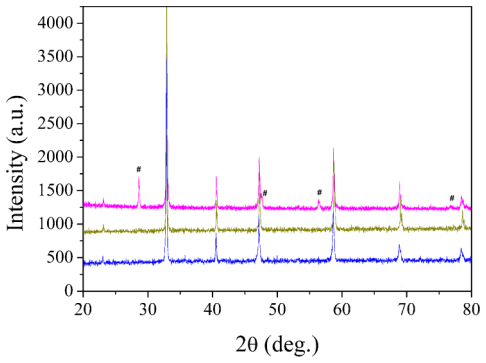

Figure 1. Powder X-ray diffraction patterns of the as-synthesized $Sr_{1-x}Ce_xCoO_{3-\delta}$ with different Ce-doping amount.

($x = 0.05$, 0.10, 0.15), abbreviated as SCCO005, SCCO010, and SCCO015 respectively hereafter. It can be seen that the SCCO005 and SCCO010 samples were phase pure, but for the nominal SCCO015 sample, a second phase marked with # was observed. As indicated in Figure 1, the second phase can be indexed to a face-centered cubic phase CeO_2 (JCPDS No. 34–0394).[12] This result indicates the solid solution limit of CeO_2 in $SrCoO_{3-\delta}$ is between 10 and 15%.

To identify the structures of $Sr_{1-x}Ce_xCoO_{3-\delta}$, the XRD pattern of the as-synthesized $Sr_{1-x}Ce_xCoO_{3-\delta}$ ($x = 0.05$ and 0.10) samples were refined in the tetragonal space group $P4/mmm$. The observed, calculated, and difference profiles together with the ascribed Bragg reflections are displayed in Figure 2. The obtained $Sr_{0.95}Ce_{0.05}CoO_{3-\delta}$ and $Sr_{0.90}Ce_{0.10}CoO_{3-\delta}$ samples are a single phase with lattice parameters a = 3.84983(5) Å, b = 3.84983(5) Å, c = 7.70711(18) Å, and a = 3.84640(4) Å, b = 3.84640(4) Å, c = 7.68366(12) Å, respectively, which are in good agreement with those reported in the literature. The lattice parameters, atomic coordinates, occupancy, and the selected bond lengths for $Sr_{1-x}Ce_xCoO_{3-\delta}$ ($x = 0.05$ and 0.10) from the powder XRD data are summarized in Table 1. It can been seen that the lattice parameters and unit-cell volume of SCCO005 are bigger than those of SCCO010 due to the larger ionic radius of Sr^{2+} (1.18 Å) compared with that of Ce^{4+} (0.97 Å),[13] indicating that Ce doping causes the lattice contraction.

The evolution of the oxygen concentration in $Sr_{0.95}Ce_{0.05}CoO_{3-\delta}$ during thermal cycling in air was determined by TGA in the temperature range of 20–900 °C with a heating/cooling rate of 2.5 °C/min. As shown in Figure 3, it can be seen that the $Sr_{0.95}Ce_{0.05}CoO_{3-\delta}$ sample experiences a weight loss at higher temperatures. Up to 700 °C, the highest temperature for electrochemical performance measurements in the present study, a weight loss of 1.9% was observed, corresponding to about 7.8% of total oxygen content. It is also noted that the oxygen loss in $Sr_{0.95}Ce_{0.05}CoO_{3-\delta}$ during high

dx.doi.org/10.1021/am3029238 | ACS Appl. Mater. Interfaces 2013, 5, 1143–1148

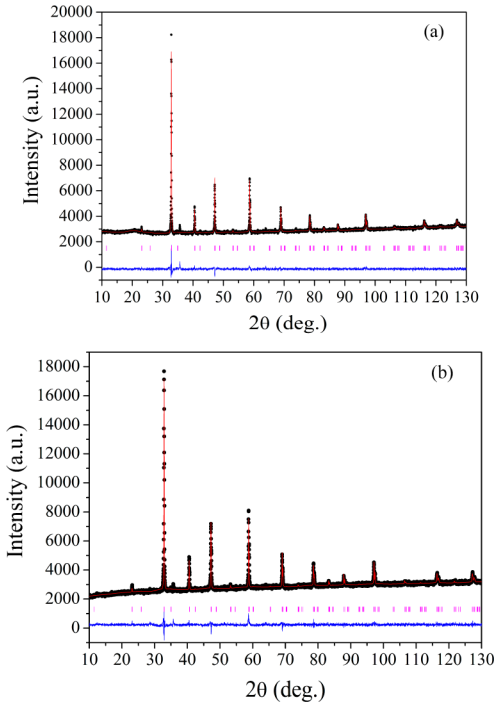

Figure 2. Observed (solid circle) and calculated (solid line) XRD patterns of $Sr_{0.95}Ce_{0.05}CoO_{3-\delta}$ (a) and $Sr_{0.90}Ce_{0.10}CoO_{3-\delta}$ (b) after refinement in the tetragonal space group *P4/mmm*. The vertical marks below the pattern give the positions of the ascribed Bragg reflections, and the difference profile is shown at the bottom.

Table 1. Lattice Parameters, Atomic Coordinates, Occupancy, and the Selected Bond Lengths for $Sr_{1-x}Ce_xCoO_{3-\delta}$ (x = 0.05 and 0.10) from the Powder XRD Data

	SCCO005	SCCO010
space group	*P4/mmm*	*P4/mmm*
a (Å)	3.84983(5)	3.84640(4)
b (Å)	3.84983(5)	3.84640(4)
c (Å)	7.70711(18)	7.68366(12)
V (Å^3)	114.228(5)	113.678(3)
d (g cm^{-3})	5.733	5.837
Ce_Ol (Å) (×4)	2.68119(4)	2.68119(4)
Ce_O2 (Å) (×4)	2.72315(4)	2.72315(4)
Ce_O3 (Å) (×4)	2.76660(4)	2.76660(4)
Col_Ol (Å)	1.92491(3) (×4)	1.92320(2)(×4)
Col_O2 (Å)	1.93680(5)(×2)	1.93090(3)(×2)
Co2_O2 (Å)	1.91676(5)(×2)	1.9I093(3)(×2)
Co2_O3 (Å)	1.92491(3)(×4)	1.92320(2)(×4)
Sr_Ol (Å)	2.68119(4)(×4)	2.67405(2)(×4)
Sr_O2 (Å)	2.72315(4)(×4)	2.72080(3)(×4)
Sr_O3 (Å)	2.76660(4)(×4)	2.76309(3)(×4)
Ol (x, 0, 0)	0.5000000(0)	0.5000000(0)
O2 (0, 0, z)	0.2513000(0)	0.2513000(0)
O3(x, 0, z)	0.5000000(0)	0.5000000(0)
R_{wp}(%)	2.04	2.20
R_p(%)	1.49	1.63

temperature is not reversible upon cooling down. The oxygen recover upon cooling down to 50 °C reached almost the same level of $Sr_{0.95}Ce_{0.05}CoO_{3-\delta}$ at 700 °C during heating.

To reveal the chemical compatibility of SCCO with ceria-based electrolyte, Figure 4 shows the XRD patterns of SDC,

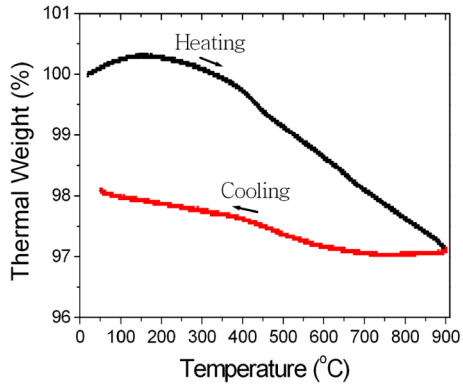

Figure 3. TGA curves of $Sr_{0.95}Ce_{0.05}CoO_{3-\delta}$ measured upon heating up and cooling down between room temperature and 900 °C in air.

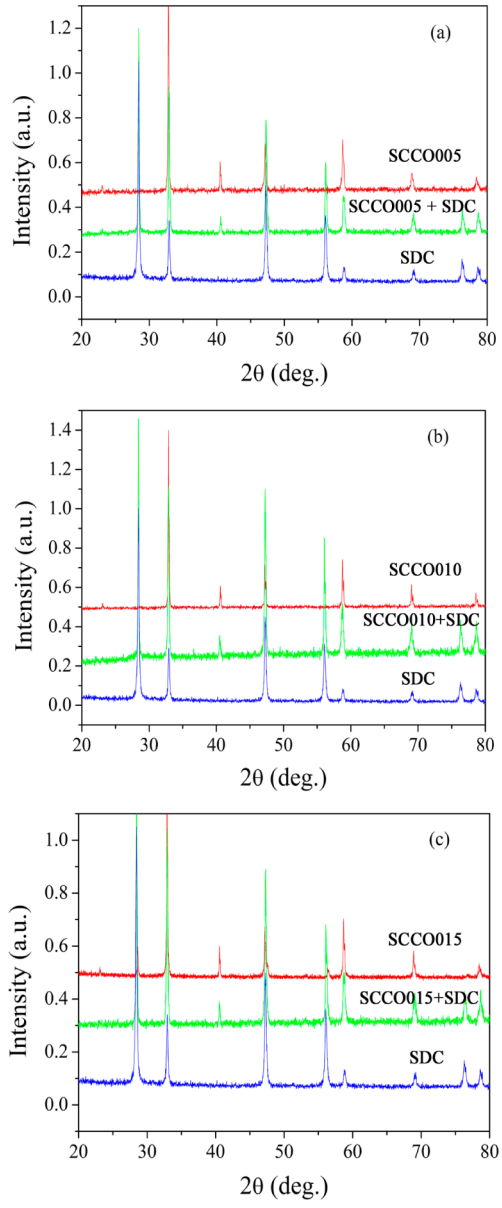

Figure 4. XRD patterns of the composites of $Sr_{1-x}Ce_xCoO_{3-\delta}$ and SDC calcined at 1000 °C for 5 h to show their chemical compatibility.

SCCO, and SDC mixed with SCCO of the same weight before and after heat treatment at 1000 °C for 5h. It clearly

dx.doi.org/10.1021/am3029238 | ACS Appl. Mater. Interfaces 2013, 5, 1143−1148

demonstrates that there is no impurity phase in the patterns, indicating that SDC and SCCO are chemically compatible at 1000 °C. Therefore, SCCO-based cathode is a potential cathode for SDC-electrolyte-based SOFCs.

3.2. Electrical Conductivity. The electrical conductivities of SCCO samples were measured in the temperature range of 400 to 800 °C using a DC four-probe configuration, as shown in Figure 5. It indicates that the electrical conductivity of

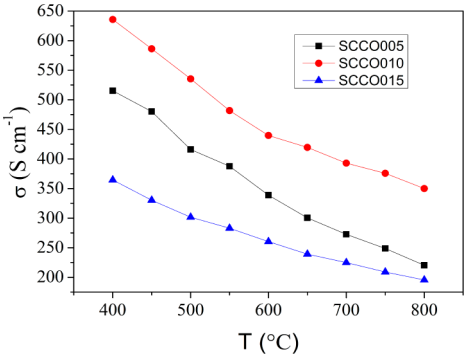

Figure 5. Electrical conductivities of $Sr_{1-x}Ce_xCoO_{3-\delta}$ (x = 0.05, 0.10, 0.15) from 400 to 800 °C measured using a DC 4-probe method.

SCCO010 is the highest among the three compositions studied, which is different with the result reported by Guo et al.[9] The three samples with different Ce-doping amount all show metallic conductivity characteristic in the temperature range of 400−800 °C. In the solid solution range that shows only perovskite phase, partial substitution of Sr by Ce in $SrCoO_{3-\delta}$ would induce the electric charge imbalance in the material.[9] Trofimenko et al.[14] found that the electrical neutrality of this material could be realized by both valence variation of B-site ions and formation of oxygen vacancies. Not only oxygen vacancies but also the transition of Co^{4+} to Co^{3+} leads to the increase in electronic hole and conductivity with increasing the doping amount of cerium. The transition from Co^{4+} to Co^{3+} would be enhanced when $x \geq 0.10$.[9] However, further increasing the doping amount of cerium will lead to the decrease in electrical conductivity due to the occurrence of CeO_2 impurity phase.

The thermal expansion coefficient of $Sr_{1-x}Ce_xCoO_{3-\delta}$ was also measured by thermal mechanical analysis as shown in Figure 6. The TECs of SCCO005 and SCCO010 samples were

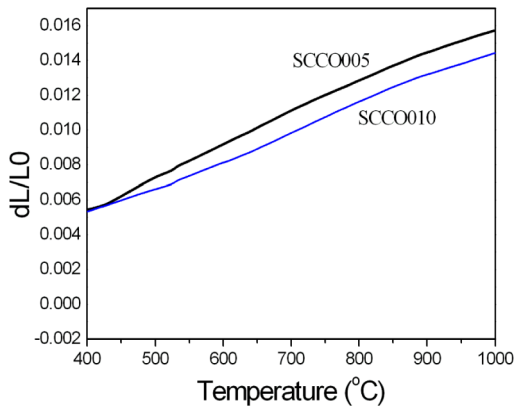

Figure 6. Thermal expansion coefficients of $Sr_{0.95}Ce_{0.05}CoO_{3-\delta}$ and $Sr_{0.90}Ce_{0.1}CoO_{3-\delta}$.

17.5×10^{-6} K^{-1} and 16.6×10^{-6} K^{-1} between 600 and 900 °C, respectively. This result shows that the TEC of SCCO is higher than those of SDC electrolyte materials (12.2×10^{-6} K^{-1}).[2] To decrease the TEC of the cathode, we studied a composite electrode consisting of SCCO and electrolyte materials in the latter section.

3.3. Polarization Resistance. An effective measure of the catalytic activity of the fuel cell cathode for oxygen reduction reactions is the area specific polarization resistance (R_p), which can be obtained from the electrochemical impedance spectroscopy (EIS) measurements on symmetric cathode fuel cells. Impedance spectra of the symmetric cells of $Sr_{1-x}Ce_xCoO_{3-\delta}$ (x = 0.05, 0.10 and 0.15) in open circuit voltage (OCV) conditions are shown in Figure 6. All the spectra were collected when the cell reached a stable state. The polarization resistance of SCCO cathodes can be calculated through the difference between the intercepts of the impedance arcs with the real axis at high frequencies and at low frequencies. To clearly show the difference in the electrode polarization behavior, the bulk resistances were removed from the spectra, showing only the cathode polarization impedances. Thus, the ASR values of the single electrode layer have been obtained from the experimentally measured values divided by two. The high-frequency arc is likely associated with an ion charge transfer process at the electrolyte−electrode interface. The high-to-intermediate frequency arc is associated with the charge transfer process at the air−electrode interface and the intermediate-to-low frequency arc is caused by oxygen surface adsorption, dissociation, and surface diffusion.[15,16] As shown in Figure 7, the SCCO010 exhibits the lowest polarization resistance from 600 to 700 °C, and only 0.23 Ω cm^2 at 700 °C, whereas the nominal SCCO015 shows the largest, consistent with the previous results that SCCO015 shows the lowest electrical conductivity and SCC010 shows the highest.

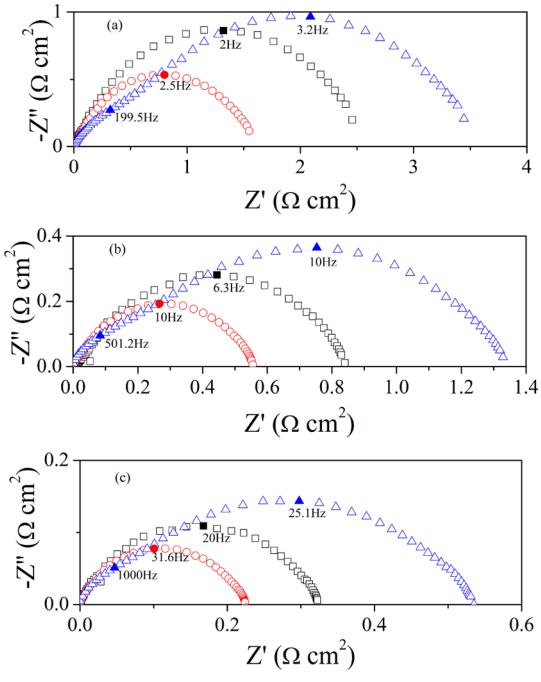

Figure 7. Impedance spectra of $Sr_{1-x}Ce_xCoO_{3-\delta}$ cathodes (□, ○, and Δ denote x = 0.05, 0.10, and 0.15, respectively) in symmetric cells with a SDC electrolyte tested at different temperatures: (a) 600, (b) 650, and (c) 700 °C.

dx.doi.org/10.1021/am3029238 | ACS Appl. Mater. Interfaces 2013, 5, 1143−1148

3.4. Single Cell Performance. Figure 8 shows the cross-sectional SEM images of the cell after the electrochemical

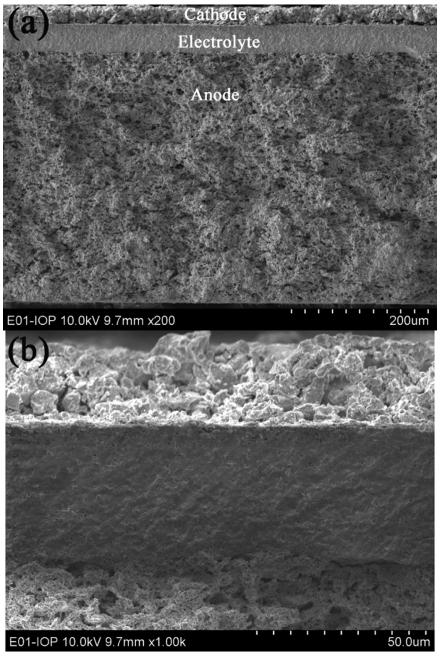

Figure 8. Cross-sectional SEM images of a single cell with a SCCO cathode, a SDC electrolyte, and a NiO-SDC composite anode: (a) overview image, and (b) high-magnification SEM image revealing the microstructural details of the electrolyte and electrodes.

testing. As seen from the image, it is clear that the three layers, cathode, electrolyte and anode, are well bonded together. The electrolyte is a dense layer with a thickness of about 44 μm. Both anode and cathode have porous microstructures with thicknesses of about 363 and 26 μm, respectively.

The electrochemical performance of $Sr_{1-x}Ce_xCoO_{3-\delta}$ (x = 0.05, 0.10, 0.15) as cathode materials was evaluated in cells Ni-SDC|SDC| SCCO. Figure 9 shows the cell voltages and power densities, as a function of current density tested in 3 wt % H_2O humidified H_2 as fuel and ambient air as oxidant at the intermediate temperature range of 600−700 °C. At 700 °C, the peak power densities of cells with $Sr_{0.95}Ce_{0.05}CoO_{3-\delta}$, $Sr_{0.90}Ce_{0.10}CoO_{3-\delta}$, and $Sr_{0.85}Ce_{0.15}CoO_{3-\delta}$ reach 0.625, 0.562, and 0.32 W cm^{-2}, respectively. Although the conductivity of $Sr_{0.90}Ce_{0.10}CoO_{3-\delta}$ is the highest, the cell with $Sr_{0.90}Ce_{0.10}CoO_{3-\delta}$ cathode did not exhibit better performance than the composition of $Sr_{0.95}Ce_{0.05}CoO_{3-\delta}$. It may be ascribed to the oxygen vacancy and Ce^{4+}/Sr^{2+} cation ordering as observed by James et al. within the ($I4/mmm$) $2a_p \times 2a_p \times 4a_p$ supercell in SCCO010,[7] which requires further studies.

It is well-known that the electrochemical reaction at the electrodes in SOFCs is generally believed to occur at the interface among gas, electronic conductor, oxygen ion conductor, which is termed the triple-phase boundary (TPB).[17,18] When the SCCO was mixed with SDC, besides effectively reducing the TEC of the cathode as mentioned above, it would also significantly extend the TPB for ORR, therefore, the composite cathodes would give enhanced performance. As shown in Figure 10, the peak power density of cells with SCCO005−30 wt % SDC is 1.01 W cm^{-2} at 700 °C, much higher than that of 0.585 W cm^{-2} for the cell with $Sm_{0.5}Sr_{0.5}CoO_3$ (SSC)-30 wt % SDC cathode and comparable

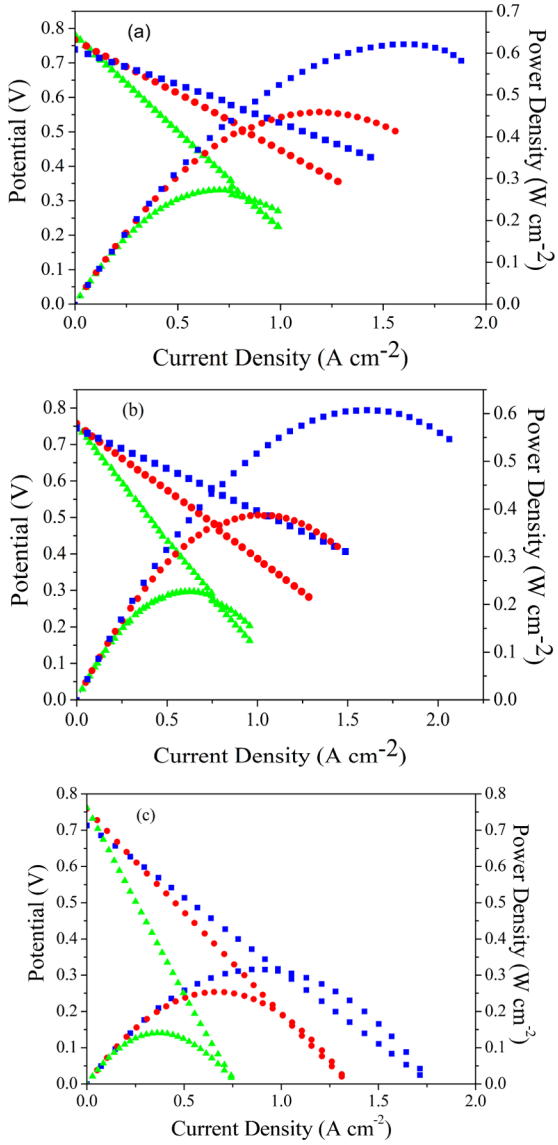

Figure 9. Cell voltage (left) and power density (right) as a function of the current density for the SDC electrolyte cell with different cathodes measured in 97% H_2-3% H_2O fuels and ambient air oxidants at 600−700 °C (■, ●, and ▲ denote 700, 650, and 600 °C, respectively.): (a) $Sr_{0.95}Ce_{0.05}CoO_{3-\delta}$, (b) $Sr_{0.90}Ce_{0.10}CoO_{3-\delta}$, and (c) $Sr_{0.85}Ce_{0.15}CoO_{3-\delta}$.

to that of the $La_{0.8}Sr_{0.2}Ga_{0.83}Mg_{0.17}O_{2.814}$ (LSGM) electrolyte cell with a $Sr_{0.7}Y_{0.3}CoO_{2.65-\delta}$ cathode reported by Goodenough et al.[19]

4. CONCLUSIONS

Perovskite $Sr_{1-x}Ce_xCoO_{3-\delta}$ ($0.05 \le x \le 0.15$) have been prepared and studied as cathodes for intermediate temperature solid oxide fuel cells. The solubility limit lies in 10−15% between $SrCoO_3$ and CeO_2. As SOFC cathodes, $Sr_{1-x}Ce_xCoO_{3-\delta}$ materials have sufficiently high electronic conductivities and excellent chemical compatibility with SDC electrolyte. The peak power density of cells Ni-SDC|SDC| $Sr_{0.95}Ce_{0.05}CoO_{3-\delta}$ is 0.625 W cm^{-2} at 700 °C. By forming a composite cathode with an oxygen ion conductor SDC, the peak power density of cell with $Sr_{0.95}Ce_{0.05}CoO_{3-\delta}$-30 wt % SDC cathode, reaches 1.01 W cm^{-2} at 700 °C, better than that of $Sm_{0.5}Sr_{0.5}CoO_3$-based cathode. All these results demonstrates

dx.doi.org/10.1021/am3029238 | ACS Appl. Mater. Interfaces 2013, 5, 1143−1148

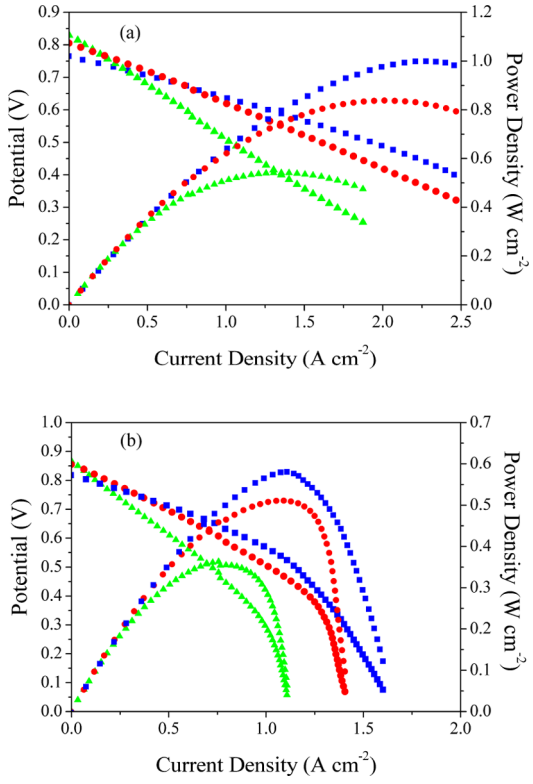

Figure 10. Characteristics of anode-supported, thin SDC electrolyte fuel cells with different composite cathodes measured in 97% H_2-3% H_2O fuel and ambient air oxidant at 600−700 °C(■, ●, and ▲ denote 700, 650, and 600 °C, respectively.): (a) $Sr_{0.95}Ce_{0.05}CoO_{3-\delta}$-30 wt % SDC, and (b) $Sm_{0.5}Sr_{0.5}CoO_3$ (SSC)-30 wt % SDC.

that $Sr_{1-x}Ce_xCoO_{3-\delta}$ ($0.05 \leq x \leq 0.15$)-based materials are promising cathodes for an IT-SOFCs.

AUTHOR INFORMATION

Corresponding Author

*E-mail: csun@iphy.ac.cn (C.S.), Xiacr@ustc.edu.cn (C.X.).

Notes

The authors declare no competing financial interest.

ACKNOWLEDGMENTS

This work is financially supported by the National Science Foundation of China (NSFC) (Grant 51172275), the National Key Basic Research Program of China (Grants 2012CB215402 and 2012CB215403), and the Institute of Physics (IOP) start-up funding for the talents. We thank Dr. Guobao Li in Peking University for the assistance and discussion in XRD refinement.

REFERENCES

(1) Sun, C. W.; Stimming, U. *J. Power Sources.* **2007**, *171*, 247−260.
(2) Sun, C. W.; Hui, R.; Roller, J. *J. Solid State Electrochem.* **2010**, *14*, 1125−1144.
(3) Hui, R.; Sun, C.; Yick, S.; Decès-Petit, C.; Zhang, X.; Maric, R.; Ghosh, D. *Electrochim. Acta* **2010**, *55*, 4772−4775.
(4) Shao, Z. P.; Haile, S. M. *Nature* **2004**, *431*, 170−173.
(5) Yan, A. Y.; Cheng, M. J.; Dong, Y. L.; Yang, W. S.; Maragou, V.; Song, S. Q.; Taiakaras, P. *Appl. Catal., B* **2006**, *66*, 64−71.
(6) Yan, A. Y.; Liu, B.; Dong, Y. L.; Tian, Z. J.; Wang, D. S.; Cheng, M. J. *Appl. Catal., B* **2008**, *80*, 24−31.
(7) James, M.; Wallwork, K. S.; Withers, R. L.; Goossens, D. J.; Wilson, K. F.; Horvat, J.; Wang, X. L.; Colella, M. *Mater. Res. Bull.* **2005**, *40*, 1415−1431.
(8) Maignan, A.; Raveau, B.; Hébert, S.; Pralong, V.; Caignaert, V.; Pelloquin, D. *J. Phys.: Condens. Mater.* **2006**, *18*, 4305−4314.
(9) Wei, Q. T.; Guo, R. S.; Wang, F. H.; Li, H. L. *J. Mater. Sci.* **2005**, *40*, 1317−1319.
(10) Larson, A. C.; Von Dreele, R. B. *General Structure Analysis System (GSAS)*; Los Alamos National Laboratory Report LAUR 86-748 ; Los Alamos National Laboratory: Los Alamos, NM, 2004.
(11) Tian, R. F.; Zha, F.; Chen, F. L.; Xia, C. R. *Solid State Ionics* **2011**, *192*, 580−583.
(12) Sun, C. W.; Li, H.; Zhang, H. R.; Wang, Z. X.; Chen, L. Q. *Nanotechnology* **2005**, *16*, 1454−1463.
(13) Shannon, R. D. *Acta Crystallogr., Sect. A* **1976**, *32*, 751−767.
(14) Trofimenko, N. E.; Ullmann, H. *J. Eur. Ceram. Soc.* **2000**, *20*, 1241−1250.
(15) Huang, C.; Chen, D.; Lin, Y.; Ran, R.; Shao, Z. *J. Power Sources* **2010**, *195*, 5176−5184.
(16) Baek, S.; Bae, J.; Yoo, Y. *J. Power Sources* **2009**, *193*, 431−440.
(17) Jiang, S. P. *Mater. Sci. Eng., A* **2006**, *418*, 199−210.
(18) Sun, C. W.; Xie, Z.; Xia, C. R.; Li, H.; Chen, L. Q. *Electrochem. Commun.* **2006**, *8*, 833−838.
(19) Li, Y.; Kim, Y. N.; Cheng, J.; Alonso, J. A.; Hu, Z.; Chin, Y.; Takami, T.; Fernandez-diaz, M. T.; Lin, H.; Chen, C.; Tjeng, L. H.; Manthiram, A.; Goodenough, J. B. *Chem. Mater.* **2011**, *23*, 5037−5044.